Journal of Pharmaceutical and Applied Chemistry

ISSN: 2357-0210 VOLUME 5, ISSUES1 , 2019 www.egyptfuture.org/ojs/

Quantum Chemical Study of the Relationships between Electronic Structure and Corticotropin-Releasing Factor 1 Receptor Binding Inhibition by a Group of Benzazole Derivatives

Abubakar Abdussalam[1,*] *and Juan S. Gómez-Jeria* [2]

[1] Department of Pure and Industrial Chemistry, Bayero University, Kano, P.M.B. 3011, Kano, Nigeria.

[2] Quantum Pharmacology Unit, Department of Chemistry, Faculty of Sciences, University of Chile. Las Palmeras 3425, Santiago 7800003, Chile.

Received: 2 Nov. 2018, Revised: 22 Dec. 2018, Accepted: 27 Dec. 2018.

Published online: 1 Jan. 2019.

Abstract: In this paper, we report the results of a study to find the relationships between electronic structure and corticotropin-releasing factor 1 receptor binding inhibition using the formal *Klopman-Peradejordi-Gómez* (KPG) method after full geometry optimization within the density functional theory (DFT) at the B3LYP/6-31g(d,p) level for a group of benzazole derivatives. Statistically significant equations were obtained. Interestingly, following the complete evaluations of the various electronic contributions of the individual molecular orbital (MO) descriptors to the binding inhibition of the benzazoles molecules investigated. The results demonstrate that the electronic interaction between the benzazole derivatives and the receptor is orbital-controlled. On the basis of the results obtained, we proposed a partial 2-dimensional pharmacophore with the contributing substituents properly positioned at the relevant molecular positions. The structural features of the proposed partial pharmacophore have the tendency to enhance its binding interaction with the receptor. The molecule-receptor interaction of the benzazoles studied herein is very complex in agreement to the high selectivity that the receptors must show to preserve the integrity of the biological system in which they are implanted.

Keywords: Benzimidazoles, QSAR, DFT, Electronic structure, Pharmacophore, Klopman-Peradejordi-Gómez method.

1 Introduction

Corticotropin-releasing hormone (CRH, also known as corticotropin-releasing factor, CRF) is a peptide hormone involved in the pathophysiology of depression [1, 2]. It is a releasing hormone belonging to the corticotropin-releasing factor family. It corresponds to a 41-amino acid peptide derived from a 196-amino acid preprohormone. CRH is secreted by the paraventricular nucleus of the mammalian hypothalamus that regulates the release of corticotropin from the pituitary gland. The CRF neuropeptide exerts its biological activity by binding to two types of CRF receptors, called CRF_1 and CRF_2. Fear-like behaviors are produced by intracerebroventricular CRF administration [3]. Research has shown that the over activity in the CRF-CRF_1 signaling system contributes to the beginning of depression and anxiety disorders. This fact has increased the clinical interest in CRH receptor antagonists that can cross the blood-brain barrier for the treatment of depression and anxiety. Several families of molecules targeting CRF_1 receptors have been synthesized and tested [4-9], and some theoretical studies were carried out [10-12].

Recently, the human CRF_1 receptor-binding activities of some benzazole derivatives were reported [8]. Considering that a better knowledge of the drug-receptor interaction will

help in the design of most potent drugs, we present in this paper the results of a quantum-chemical study of the relationships between electronic structure and CRF_1 receptor inhibition by a set of the above mentioned benzazole derivatives.

2 Experimental

2.1 Methods, Models and Calculations

The selected molecules are a group of benzazole derivatives and were selected from a recent study[8]. Their general structure and biological activity are displayed, respectively, in Fig. 1 and Table 1. The activity selected for this study is the inhibitory activity against ovine ^{125}I-CRF binding to human CRF_1 receptors expressed on Chinese hamster ovary cellular membranes [8].

Table 1: Benzazole derivatives and CRF_1 receptor binding inhibition activities.

S/N	[a]Mol.	R_1	R_2	R_3	R_4	R_5	R_6	R_7	R_8	Log(IC_{50})
1	5	*n*-Pr	*n*-Pr	H	H	Me	Me	Me	-	2.30
2	9	*n*-Pr	*n*-Pr	H	H	Me	Me	Me	-	1.89
3	13	*n*-Pr	*n*-Pr	H	H	Me	Me	Me	H	3.40
4	22a	*n*-Pr	*n*-Pr	H	H	Me	Me	Me	Me	1.18
5	22b	*n*-Pr	*n*-Pr	H	H	Me	Me	Me	*i*-Pr	1.99
6	22c	*n*-Pr	*n*-Pr	H	H	Me	Me	Me	Ph	3.34
7	29a	*n*-Pr	*n*-Pr	H	H	H	Me	Me	Me	1.15
8	29b	*n*-Pr	*n*-Pr	H	H	Me	Me	H	Me	1.18
9	29c	*n*-Pr	*n*-Pr	H	H	Me	OMe	Cl	Me	1.04
10	29d	*n*-Pr	*n*-Pr	H	H	Me	OMe	Br	Me	1.92
11	29e	*n*-Pr	*n*-Pr	H	H	Me	*i*-Pr	Cl	Me	2.15
12	29f	Et	Et	H	H	Me	OMe	Br	Me	1.15
13	22d	*n*-Bu	*n*-Bu	H	H	Me	OMe	Br	Me	1.08
14	23	*i*-Pr	Et	H	H	Me	OMe	Br	Me	1.34
15	22e	MeOEt	MeOEt	H	H	Me	OMe	Br	Me	1.11
16	29g	*n*-Pr	*n*-Pr	H	Cl	Me	OMe	Cl	Me	0.98
17	29h	*n*-Pr	*n*-Pr	Cl	Cl	Me	OMe	Cl	Me	2.23
18	29j	*n*-Pr	*n*-Pr	H	CN	Me	OMe	Cl	Me	1.15
19	29k	Et	Et	H	Cl	Me	OMe	Cl	Me	1.38
20	29l	Et	Et	H	CN	Me	OMe	Cl	Me	1.14
21	29m	Et	Et	H	Me	Me	OMe	Cl	Me	0.88
22	29o	Et	Et	H	OMe	Me	OMe	Cl	Me	1.11

[a]Mol. = Molecule

The electronic structure of all molecules was calculated within the Density Functional Theory (DFT) at the B3LYP/6-31g(d,p) level after full geometry optimization[13]. The Gaussian collection of programs was used[14]. All the information needed to calculate numerical values for the local atomic reactivity indices was obtained from the Gaussian results with the D-Cent-QSAR software[15]. All the electron populations smaller than or equal to 0.01 e were considered as zero[16].

Negative electron populations coming from Mulliken Population Analysis were corrected as usual[16]. Since the resolution of the system of linear equations is not possible because we have not enough molecules, we employed Linear Multiple Regression Analysis (LMRA) techniques to find the best solution. A matrix containing the dependent variable (log(IC50) value of each case) and the local atomic reactivity indices of all atoms of the common skeleton as independent variables was built[17] The Statistica software was used for LMRA[18].

We worked with the *common skeleton hypothesis* defined as a definite collection of atoms, common to all molecules

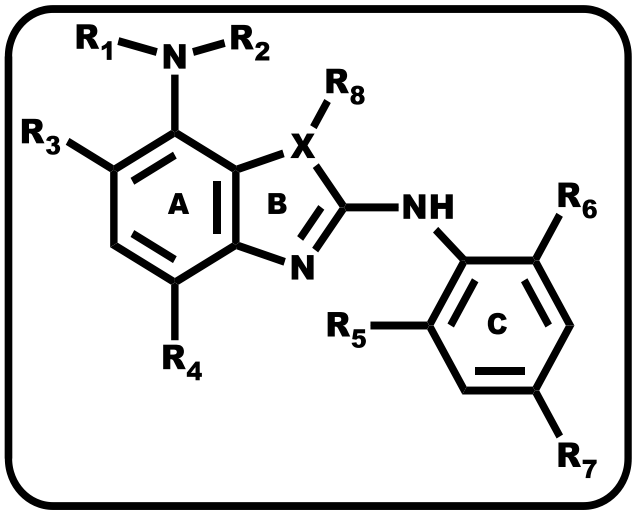

Fig. 1: General structure of the benzazole derivatives.

analyzed. The action of the substituents consists in modifying the electronic structure of the common skeleton and influencing the right alignment of the drug throughout the orientational parameters. It is hypothesized that different parts or this common skeleton accounts for almost all the interactions leading to the expression of a given biological activity. The common skeleton is shown in Fig. 2.

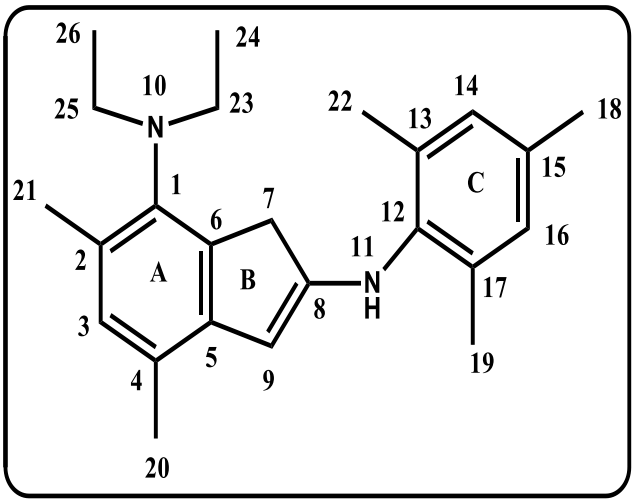

Fig. 2: Common skeleton numbering of the molecules.

The KPG (Klopman-Peradejordi-Gómez) method was employed for obtaining the formal structure-activity relationship. Considering that this method has been extensively explained in earlier papers, we refer the reader to that literature [17], [19-23]. KPG method has shown its potency and explanatory characteristics in a large number of different families of molecules and many biological activities [24-34].

3 Results

The best equation obtained is:

$$\log(IC_{50}) = 1.72 - 8.84F_{19}(\text{LUMO})^* + 0.61S_{22}^{N}(\text{LUMO})^* + 3.70F_{20}(\text{LUMO})^* - 2.36F_{9}(\text{LUMO}+1)^* - 1.23S_{6}^{E}(\text{HOMO}-2)^* \quad (1)$$

With n=21, R=0.97, R^2=0.94, adj-R^2=0.92, F(5,15)=47.25 (p<0.000001) and SD=0.21. No outliers were detected and no residuals fall outside the ±2σ limits. Here, F_{19}(LUMO)* is the electron population (or Fukui index) of the lowest empty MO localized on atom 19, S_{22}^{N}(LUMO)* is the nucleophilic superdelocalizability of the lowest empty MO localized on atom 22, F_{20}(LUMO)* is the electron population of the lowest empty MO localized on atom 20, F_9(LUMO+1)* is the electron population of the second lowest empty MO localized on atom 9 and S_6^E(HOMO-2)* is the electrophilic superdelocalizability of the third highest occupied MO localized on atom 6. Table 2 and 3 show the beta coefficients, the results of the t-test for significance of coefficients and the matrix of squared correlation coefficients for the variables of Eq. 1. There are no significant internal correlations between independent

variables (Table 3). Figure 3 displays the plot of observed *vs.* predicted

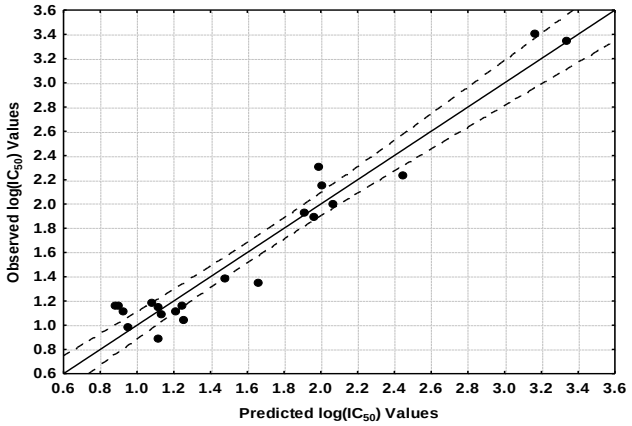

Fig. 3: Plot of predicted *vs*. observed log(IC_{50}) values (Eq. 1). Dashed lines denote the 95% confidence interval. calculated log(IC_{50}) values.

3.1 Local Molecular Orbitals

Tables 4 and 5 shows the local MO structure of atoms 6, 9, 19, 20 and 22 (see Fig. 2). Nomenclature: Molecule (HOMO) / (HOMO-2)* (HOMO-1)* (HOMO)* - (LUMO)* (LUMO+1)* (LUMO+2)*.

3.2 Discussion

A very important point to stress is the following. When a local atomic reactivity index of an inner occupied MO (i.e., HOMO-1 and/or HOMO-2) or of a higher vacant MO (LUMO+1 and/or LUMO+2) appears in any equation, this means that the remaining of the upper occupied MOs (for example, if HOMO-2 appears, upper means HOMO-1 and HOMO) or the remaining of the empty MOs (for example, if LUMO+1 appears, lower means the LUMO) contribute to the interaction[17]. Table 2 shows that the importance of

Table 2: Beta coefficients and t-test for significance of coefficients in Equation 1

MO Descriptor	Beta	t(15)	p-level
F_{19}(LUMO)*	-0.39	-5.04	0.0001
S_{22}^{N}(LUMO)*	0.76	8.73	0.000000
F_{20}(LUMO)*	0.24	3.55	0.003
F_{9}(LUMO+1)*	-0.30	-4.07	0.001
S_{6}^{E}(HOMO-2)*	-0.26	-3.45	0.004

Table 3: Matrix of squared correlation coefficients for the variables in Eq. 1.

MO Descriptor	F_{19}(LUMO)*	S_{22}^{N}(LUMO)*	F_{20}(LUMO)*	F_{9}(LUMO+1)*
F_{19}(LUMO)*	1.00			
S_{22}^{N}(LUMO)*	0.21	1.00		
F_{20}(LUMO)*	0.00	0.00	1.00	
F_{9}(LUMO+1)*	0.04	0.09	0.01	1.00
S_{6}^{E}(HOMO-2)*	0.04	0.17	0.12	0.00

Table 4: Local Molecular Orbitals of atoms 6, 9 and 19.

Mol.	Atom 6	Atom 9	Atom 19
1(95)	93π94π95π-98π99π100π	91π94π95π-96π98π99π	85σ87σ92σ-96π109π110π
2(99)	97π98π99π-100σ102σ103π	97π98π99π-100σ102π103π	93σ96σ97σ-117σ121σ123σ
3(95)	93π94σ95π-98π99π100π	93π94π95π-96π98π99π	82σ84σ91σ-103σ106π107π
4(99)	97σ98π99σ-102π103π104π	97π98π99π-100π102π103π	89σ90σ95σ-101σ108σ112π
5(107)	105π106π107π-110π111π112σ	103π106π107π-108π112π113π	96σ99σ104σ-108π109σ113π
6(115)	111π114π115σ-116σ117σ120π	113π114π115π-116π117π118π	107σ111σ112σ-132σ133σ134π
7(99)	97σ98π99π-102π103π104σ	97π98π99π-100π102π103π	89σ90σ95σ-101σ108σ112π
8(95)	93σ94σ95σ-98π99π100σ	93π94π95π-96π98π99π	85σ86σ91σ-97σ104σ109σ
9(107)	104σ105π106π-110π111π112π	105π106π107π-108π110π112π	104π105π106π-109π111σ125π
10(116)	114π115π116π-119π121π122π	113π115π116π-117π121π123π	114π115π116π-118π119π120σ
11(111)	109σ110π111π-114π115π116π	106σ109π111π-112π114π117π	103σ104σ107σ-113σ126σ131σ
12(108)	106π107π108σ-112π113π114σ	106π107π108π-109π112π113π	105π106π107π-110π111σ118σ
13(124)	122σ123σ124π-126π127π129π	122π123σ124σ-125π129π131π	121π122π124π-126π127π128σ
14(116)	114π115π116π-120π121π122σ	114π115π116π-117σ120π121π	113π114π115π-118π119σ127σ
15(124)	122π123π124π-128π129π130σ	121π123π124π-125π128π129π	122π123π124π-126π127σ136σ
16(115)	113σ114π115π-118π119π121σ	110σ114π115σ-116π119π121σ	111π112π115π-117σ120σ127σ
17(123)	121σ122σ123π-125π126π127π	121σ122π123σ-124π127π130π	119π120π123π-125π126π129σ
18(113)	111σ112π113π-114π115π117π	111π112π113π-114π115π117π	110π111π113π-116π118σ126σ
19(103)	101π102π103π-106π107π109σ	98π99π103π-104π106π107π	94π100π101π-105π162σ169σ
20(105)	103π104π105σ-106π107π109π	102π104π105π-106π111π113π	101π103π104π-108π110σ124π
21(103)	101π102π103π-104π106π108π	100π102π103π-104π105π106π	100π101π102π-105π107σ112σ
22(107)	105σ106π107π-110π112π113π	102σ106π107π-108π110π112π	103π104π106π-109π111σ117σ

Table 5: Local Molecular Orbitals of atoms 20 and 22.

Mol.	Atom 20	Atom 22
1(95)	84σ86σ90σ- 102π106π107π	89π92σ93σ- 104π106π108π
2(99)	85σ90σ91σ- 104σ109σ114σ	88σ89σ96σ- 113σ114σ115σ
3(95)	79σ80σ90σ- 108π109π111π	84σ88σ91σ- 103σ111π114σ
4(99)	83σ89σ94σ- 106σ108σ109σ	90σ92σ95σ- 110σ111σ114σ
5(107)	89σ90σ100σ- 117π119σ120σ	96σ99σ104σ- 110σ119σ124σ
6(115)	96σ98σ110σ- 124π129σ130σ	103σ105σ111σ- 119σ131σ132σ
7(99)	83σ89σ94σ- 106σ108σ109σ	90σ92σ95σ- 110σ111σ114σ
8(95)	85σ86σ90σ- 102σ105σ106π	86σ88π91σ- 104σ106σ107σ
9(107)	93σ97σ102σ- 118σ119σ123σ	98σ99σ103σ- 108σ111σ119σ
10(116)	99σ103σ111σ- 124σ125σ126σ	107σ108σ112σ- 117σ120σ130σ
11(111)	92σ93σ106σ- 122σ124σ127σ	102σ103σ107σ- 112σ116σ126σ
12(108)	92σ96 σ103σ- 117σ118π119σ	98σ99σ104σ- 109σ111σ120σ
13(124)	109σ113σ119σ- 133σ136σ137σ	115σ116σ120- 125σ128σ138σ
14(116)	99σ102σ111σ- 128σ131σ134σ	105σ102σ112σ- 117σ119σ127σ
15(124)	107σ108σ118σ- 136π137σ141σ	110σ113σ120σ- 125σ127σ138σ
16(115)	110σ114π115π- 118π121σ126σ	105σ106σ111σ- 116σ120σ128σ
17(123)	121π122π123π- 124π125π128σ	112σ113σ119σ- 129σ137σ140σ
18(113)	107π108σ112π- 114π115π119π	103σ104σ109σ- 115σ118σ128σ
19(103)	99π102π103π- 106π110σ111σ	93σ94σ100σ- 104σ108σ115σ
20(105)	99π100σ102π- 106π107π111π	95σ96σ101σ- 110σ117σ119σ
21(103)	97σ98σ103π- 106σ127σ128σ	90σ93σ94σ- 104σ107σ114σ
22(107)	102σ105π107π- 110π112π127σ	98σ99σ103σ- 108σ111σ118σ

variables in Eq. 1 is S_{22}^{N}(LUMO)* > F_{19}(LUMO)* > F_9(LUMO+1)* > S_6^{E}(HOMO-2)* > F_{20}(LUMO)*. A high inhibitory activity is associated with high (positive) values of F_{19}(LUMO)* and F_9(LUMO+1)*, with small (positive) values of S_{22}^{N}(LUMO)* and F_{20}(LUMO)*; and with small (negative) values of S_6^{E}(HOMO-2)*. Now we shall employ the variable-by-variable analysis of Eq. 1 to get an approximate idea of what is the role of the atoms appearing there[23].

Atom 22 is the atom of the substituent directly bonded to atom 13 (R_5, Fig. 2). Table 1 shows that this substituent is apolar (hydrophobic) volume exists in the receptor site, constituted by methanediyl groups from some amino acids. Atom 19 is the atom of the substituent directly bonded toH or Me only. Table 5 shows that all MOs have a σ character. A high inhibitory activity is associated with small (positive) values of S_{22}^{N}(LUMO)*. Small values are obtained by shifting upwards the $LUMO_{22}^{*}$ energy, making this MO less reactive. Note that $LUMO_{22}^{*}$ and $HOMO_{22}^{*}$ are energetically far from the molecule's frontier MOs. Therefore we may preclude a direct charge transfer. With these considerations we suggest that atom 22 is probably engaged in a weak filled-MO/empty-MO interaction with a site having empty σ MOs available. This implies that an atom 17 (R_6, Fig. 2). Table 4 shows that all MOs have a σ character and that $LUMO_{19}^{*}$ and $HOMO_{19}^{*}$ are energetically far from the molecule's frontier MOs. Therefore, direct charge transfer is excluded. A high inhibitory activity is associated with high (positive) values of F_{19}(LUMO)*, suggesting immediately that atom 19 is interacting weakly with a filled σ MO of the receptor.

Atom 9 is a carbon in ring B (Fig. 2). Table 4 shows that the local frontier molecular orbitals, $HOMO_9^{*}$ and $LUMO_9^{*}$, coincide with the molecular frontier MOs in all cases. All these MOs have a π nature. A high inhibitory

activity is associated with high (positive) values of F_9(LUMO+1)*. This suggests that atom 9 is interacting with an electron-rich center through at least its two lowest empty local MOs.

Atom 6 is a carbon belonging to rings A and B (Fig. 2). Table 4 shows that the local HOMO, $HOMO_6^{*}$, coincides with the molecular HOMO in all but one molecule. The three highest occupied local MOs have different natures, σ or π, following the molecule. Small negative values of S_6^{E}(HOMO-2)* are associated with high activity. This means a low electron-donor capacity of this local MO. On the other hand, atom 6 has a positive net charge in all molecules. We may interpret these results by suggesting that atom 6 is interacting weakly with an electron-rich center. Given that the lowest empty local MOs of atom 6 do not coincide with the molecular equivalents and that the nature of them is also σ or π following the molecule, we cannot specify what kind of interaction could be in action.

Atom 20 is the first atom of the substituent linked to atom 4 (Fig. 2 and Table 1). Small values F_{20}(LUMO)* are associated with high activity. Table 5 shows that $(LUMO)_{20}^{*}$ has π or σ natures following the molecule, and that the local frontier MOs correspond to inner occupied and highest empty molecular MOs. This allows us to suggest that this atom is engaged in a weak interaction with an electron-rich center of unknown nature. But we may say that this center is able to interact with π and σ electrons. All the suggestions are displayed in the partial 2D pharmacophore of Fig. 4.

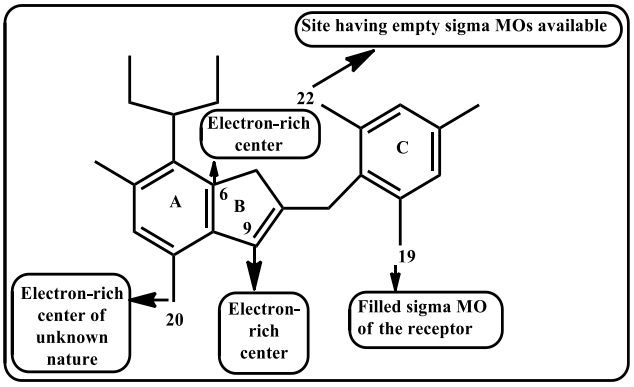

Fig. 4: 2D partial pharmacophore for corticotropin-releasing Factor 1 receptor binding inhibition.

References

[1] Roberto, M.; Spierling, S. R.; Kirson, D.; Zorrilla, E. P. Chapter Two - Corticotropin-Releasing Factor (CRF) and Addictive Behaviors. *International Review of Neurobiology*, Thiele, T. E., Ed. Academic Press., **136**, 5-51(2017).

[2] Davis, E. G.; Keller, J.; Hallmayer, J.; Pankow, H. R.; Murphy, G. M.; Gotlib, I. H.; Schatzberg, A. F. Corticotropin-releasing factor 1 receptor haplotype and cognitive features of major depression. *Translational Psychiatry.*, **8**, 5(2018).

[3] Meloni, E. G.; Gerety, L. P.; Knoll, A. T.; Cohen, B. M.; Carlezon, W. A. Behavioral and Anatomical

Interactions between Dopamine and Corticotropin-Releasing Factor in the Rat. *The Journal of Neuroscience.*, **26**, 3855(2006).

[4] Kojima, T.; Mochizuki, M.; Takai, T.; Hoashi, Y.; Morimoto, S.; Seto, M.; Nakamura, M.; Kobayashi, K.; Sako, Y.; Tanaka, M.; Kanzaki, N.; Kosugi, Y.; Yano, T.; Aso, K. Discovery of 1,2,3,4-tetrahydropyrimido[1,2-a]benzimidazoles as novel class of corticotropin releasing factor 1 receptor antagonists. *Bioorganic & Medicinal Chemistry* 2018.

[5] Teleb, M.; Kuppast, B.; Spyridaki, K.; Liapakis, G.; Fahmy, H. Synthesis of 2-imino and 2-hydrazono thiazolo[4,5-d]pyrimidines as corticotropin releasing factor (CRF) antagonists. *European Journal of Medicinal Chemistry.*, **138**, 900-908(2017).

[6] Mochizuki, M.; Kojima, T.; Kobayashi, K.; Kotani, E.; Ishichi, Y.; Kanzaki, N.; Nakagawa, H.; Okuda, T.; Kosugi, Y.; Yano, T.; Sako, Y.; Tanaka, M.; Aso, K. Discovery of 4-chloro-2-(2,4-dichloro-6-methylphenoxy)-1-methyl-7-(pentan-3-yl)-1H-benzimidazole, a novel CRF1 receptor antagonist. *Bioorganic & Medicinal Chemistry.*, **25**, 1556-1570(2017).

[7] Mochizuki, M.; Kori, M.; Kono, M.; Yano, T.; Sako, Y.; Tanaka, M.; Kanzaki, N.; Gyorkos, A. C.; Corrette, C. P.; Aso, K. Discovery of a 7-arylaminobenzimidazole series as novel CRF1 receptor antagonists. *Bioorganic & Medicinal Chemistry.*, **24**, 4675-4691(2016).

[8] Mochizuki, M.; Kori, M.; Kobayashi, K.; Yano, T.; Sako, Y.; Tanaka, M.; Kanzaki, N.; Gyorkos, A. C.; Corrette, C. P.; Cho, S. Y.; Pratt, S. A.; Aso, K. Design and Synthesis of Benzimidazoles As Novel Corticotropin-Releasing Factor 1 Receptor Antagonists. *Journal of Medicinal Chemistry.*, **59**, 2551-2566(2016).

[9] Han, X.; Pin, S. S.; Burris, K.; Fung, L. K.; Huang, S.; Taber, M. T.; Zhang, J.; Dubowchik, G. M. Synthesis and structure–activity relationship of imidazo[1,2-a]benzimidazoles as corticotropin-releasing factor 1 receptor antagonists. *Bioorganic & Medicinal Chemistry Letters.*, **15**, 4029-4032(2005).

[10] Shekhar Mishra, S.; Venkatachalam, T.; Shekhar Sharma, C.; Pratap Singh, H.; Kalra, S.; Kumar, N. Computational investigation of binding mechanism of substituted pyrazinones targeting corticotropin releasing factor-1 receptor deliberated for anti-depressant drug design. *Journal of Biomolecular Structure and Dynamics.*, 1-39(2018).

[11] Kumar, N.; Mishra, S. S.; Sharma, C. S.; Singh, H. P.; Kalra, S. In silico binding mechanism prediction of benzimidazole based corticotropin releasing factor-1 receptor antagonists by quantitative structure activity relationship, molecular docking and pharmacokinetic parameters calculation. *Journal of Biomolecular Structure and Dynamics.*, **36**, 1691-1712(2018).

[12] Kumar, N.; Mishra, S. S.; Sharma, C. S.; Singh, H. P.; Kalra, S. In silico binding mechanism prediction of benzimidazole based corticotropin releasing factor-1 receptor antagonists by quantitative structure activity relationship, molecular docking and pharmacokinetic parameters calculation. *Journal of Biomolecular Structure and Dynamics.*, 1-22(2017).

[13] Note. The results presented here are obtained from what is now a routinary procedure. For this reason, we built a general model for the paper's structure. This model contains standard phrases for the presentation of the methods, calculations and results because they do not need to be rewritten repeatedly and the number of possible variations to use is finite. In 2017.

[14] Frisch, M. J.; Trucks, G. W.; Schlegel, H. B.; Scuseria, G. E.; Robb, M. A.; Cheeseman, J. R.; Montgomery, J., J.A.; Vreven, T.; Kudin, K. N.; Burant, J. C.; Millam, J. M.; Iyengar, S. S.; Tomasi, J.; Barone, V.; Mennucci, B.; Cossi, M.; Scalmani, G.; Rega, N. *G03 Rev. E.01, Gaussian*: Pittsburgh, PA, USA, 2007.

[15] Gómez-Jeria, J. S. D-Cent-QSAR: A program to generate Local Atomic Reactivity Indices from Gaussian 03 log files. v. 1.0, v. 1.0; Santiago, Chile, 2014.

[16] Gómez-Jeria, J. S. An empirical way to correct some drawbacks of Mulliken Population Analysis (Erratum in: J. Chil. Chem. Soc., 55, 4, IX, 2010). *Journal of the Chilean Chemical Society.*, **54**, 482-485(2009).

[17] Gómez-Jeria, J. S. 45 Years of the KPG Method: A Tribute to Federico Peradejordi. *Journal of Computational Methods in Molecular Design.*, **7,** 17-37(2017).

[18] Statsoft. Statistica v. 8.0, 2300 East 14 th St. Tulsa, OK 74104, USA, 1984-2007.

[19] Gómez Jeria, J. S. La Pharmacologie Quantique. *Bollettino Chimico Farmaceutico.*, **121**, 619-625(1982).

[20] Gómez-Jeria, J. S. On some problems in quantum pharmacology I. The partition functions. *International Journal of Quantum Chemistry.*, **23**, 1969-1972(1983).

[21] Gómez-Jeria, J. S. Modeling the Drug-Receptor Interaction in Quantum Pharmacology. In Molecules in Physics, Chemistry, and Biology, Maruani, *J., Ed. Springer* Netherlands., **4**, 215-231(1989).

[22] Gómez-Jeria, J. S.; Ojeda-Vergara, M. Parametrization of the orientational effects in the drug-receptor interaction. *Journal of the Chilean Chemical Society.*, **48**, 119-124(2003).

[23] Gómez-Jeria, J. S.; Kpotin, G. Some Remarks on The Interpretation of The Local Atomic Reactivity Indices Within the Klopman-Peradejordi-Gómez (KPG) Method. I. Theoretical Analysis. Research *Journal of Pharmaceutical, Biological and Chemical Sciences.*, **9**, 550-561(2018).

[24] Gómez-Jeria, J. S.; Moreno-Rojas, C.; Castro-Latorre, P. A note on the binding of N-2-methoxybenzyl-phenethylamines (NBOMe drugs) to the 5-HT2C receptors. *Chemistry Research Journal.*, **3**, 169-175 (2018).

[25] Gómez-Jeria, J. S.; Castro-Latorre, P.; Moreno-Rojas, C. Dissecting the drug-receptor interaction with the Klopman-Peradejordi-Gómez (KPG) method. II. The interaction of 2,5-dimethoxyphenethylamines and their N-2-methoxybenzyl-substituted analogs with 5-HT2A serotonine receptors. *Chemistry Research Journal.*, **4**, 45-62(2018).

[26] Kpotin, G.; Gómez-Jeria, J. S. A Quantum-chemical Study of the Relationships Between Electronic Structure and Anti-proliferative Activity of Quinoxaline Derivatives on the HeLa Cell Line. *International Journal of Computational and Theoretical Chemistry.*, **5**, 59-68(2017).

[27] Gómez-Jeria, J. S.; Surco-Luque, J. C. A Quantum Chemical Analysis of the Relationships between Electronic Structure and the inhibition of Botulinum Neurotoxin serotype A by a series of Derivatives possessing an 8-hydroxyquinoline core. *Chemistry Research Journal.*, **2,** 1-11(2017).

[28] Gómez-Jeria, J. S.; Moreno-Rojas, C. Dissecting the drug-receptor interaction with the Klopman-Peradejordi-Gómez (KPG) method. I. The interaction of 2,5-dimethoxyphenethylamines and their N-2-methoxybenzyl-substituted analogs with 5-HT1A serotonine receptors. *Chemistry Research Journal*., **2**, 27-41(2017).

[29] Gómez-Jeria, J. S.; Castro-Latorre, P.; Kpotin, G. Quantum Chemical Study of the Relationships between Electronic Structure and Antiviral Activities against Influenza A H1N1, Enterovirus 71 and Coxsackie B3 viruses of some Pyrazine-1,3-thiazine Hybrid Analogues. *International Journal of Research in Applied, Natural and Social Sciences.*, **5**, 49-64(2017).

[30] Gómez-Jeria, J. S.; Castro-Latorre, P. A Density Functional Theory analysis of the relationships between the Badger index measuring carcinogenicity and the electronic structure of a series of substituted Benz[a]anthracene derivatives. *Chemistry Research Journal.*, **2**, 112-126(2017).

[31] Gómez-Jeria, J. S.; Becerra-Ruiz, M. B. Electronic structure and rat fundus serotonin receptor binding affinity of phenetylamines and indolealkylamines. *International Journal of Advances in Pharmacy, Biology and Chemistry.*, **6**, 72-86(2017).

[32] Gómez-Jeria, J. S.; Abuter-Márquez, J. A Theoretical Study of the Relationships between Electronic Structure and 5-HT1A and 5- HT2A Receptor Binding Affinity of a group of ligands containing an isonicotinic nucleus. *Chemistry Research Journal.*, **2**, 198-213(2017).

[33] Anatovi, W.; Kpotin, G.; Kuevi, U. A.; Houngue-Kpota, A.; Atohoun, G. S.; Mensah, J.-B.; Gómez-Jeria, J. S. A DFT study or the relationship between the electronic structure and the antiplasmodial activity of a series of 4-anilino-2-trichloromethylquinazolines derivatives. *World Scientific News.* **88**, 138-151(2017).

[34] Robles-Navarro, A.; Gómez-Jeria, J. S. A Quantum-Chemical Analysis of the Relationships between Electronic Structure and Citotoxixity, GyrB inhibition, DNA Supercoiling inhibition and anti-tubercular activity of a series of quinoline–aminopiperidine hybrid analogues. *Der Pharma Chemica.*, **8**, 417-440(2016).